Resonant States in ^{5}He and ^{5}Li and Nucleon-α Scattering

A. I. Mazur[a], A. M. Shirokov[a,b,c], I. A. Mazur[a], E. A. Mazur[a], Y. Kim[d], I. J. Shin[d], L. D. Blokhintsev[a,b] and J. P. Vary[c]

[a] *Department of Physics, Pacific National University, Khabarovsk 680035, Russia*
[b] *Skobeltsyn Institute of Nuclear Physics, Lomonosov Moscow State University, Moscow 119991, Russia*
[c] *Department of Physics and Astronomy, Iowa State University, Ames, IA 50011-3160, USA*
[d] *Rare Isotope Science Project, Institute for Basic Science, Daejeon 305-811, Korea*

Abstract

The SS-HORSE approach to analysis of resonant states is generalized to the case of charged particle scattering utilizing analytical properties of partial scattering amplitudes and applied to the study of resonant states in the ^{5}Li nucleus and non-resonant s-wave proton-α scattering within the no-core shell model using the JISP16 and Daejeon16 NN interactions.

Keywords: *Charged particle scattering; resonances; scattering amplitude; effective range function; SS-HORSE approach; no-core shell model*

1 Introduction

There is considerable progress in developing *ab initio* methods for studying nuclear structure [1] based on a rapid development of supercomputer facilities and recent advances in the utilization of high-performance computing systems. In particular, modern *ab initio* approaches, such as the Green's Function Monte Carlo (GFMC) [2], the Hyperspherical expansion [1], the No-Core Shell Model (NCSM) [3], the Coupled-Cluster Theory [4, 5], and the Nuclear Lattice Effective Field Theory [6, 7] are able to reproduce properties of atomic nuclei with mass up to $A = 16$ and selected heavier nuclear systems around closed shells.

Within NCSM as well as within other shell model approaches, the calculation of nuclear ground states and other bound states starts conventionally from estimating the $\hbar\Omega$ dependence of the energy $E_\nu(\hbar\Omega)$ of the bound state ν in some model space. The minimum of $E_\nu(\hbar\Omega)$ is correlated with the energy of the state ν. The convergence of calculations and accuracy of the energy prediction is estimated by comparing with the results obtained in neighboring model spaces. To improve the accuracy of theoretical predictions, various extrapolation techniques have been suggested recently [8–19] which make it possible to estimate the binding energies in the complete infinite shell-model basis space. The studies of extrapolations to the infinite model spaces reveal general trends of convergence patterns of shell model calculations.

Proceedings of the International Conference 'Nuclear Theory in the Supercomputing Era — 2016' (NTSE-2016), Khabarovsk, Russia, September 19–23, 2016. Eds. A. M. Shirokov and A. I. Mazur. Pacific National University, Khabarovsk, Russia, 2018, p. 185.

http://www.ntse-2016.khb.ru/Proc/AMazur.pdf.

An extension of the *ab initio* methods to the studies of the continuum spectrum and nuclear reactions is one of the mainstreams of modern nuclear theory. A remarkable success in developing the *ab initio* reaction theory was achieved in few-body physics where exact Faddeev and Faddeev–Yakubovsky equations [20] or the AGS method [21] are nowadays routinely used for calculating various few-body reactions.

The most important breakthrough in developing *ab initio* theory of nuclear reactions in systems with total number of nucleons $A > 4$ was achieved by combining NCSM and Resonating Group Method (RGM); the resulting approach is conventionally referred to as NCSM/RGM or No-Core Shell Model with Continuum (NCSMC) [3, 22–24]. It is also worth noting the Lorentz integral transform approach to nuclear reactions with electromagnetic probes [1, 25] and the GFMC calculations of elastic $n\alpha$ scattering [26]. Nuclear resonance can be also studied within the No-core Gamow Shell Model (NCGSM) [27].

Both NCGSM and NCSM/RGM complicate essentially the shell model calculations. A conventional belief is that the energies of shell model states in the continuum should be associated with the resonance energies. It was shown however in Refs. [28, 29] that the energies of shell model states may appear well above the energies of resonant states, especially for broad resonances. Moreover, the analysis of Refs. [28, 29] clearly demonstrated that the shell model should also generate some states in a non-resonant nuclear continuum. In Refs. [30–34] we suggested an SS-HORSE approach which provides an interpretation of the shell model states in the continuum and makes it possible to deduce resonance energies and width or low-energy non-resonant phase shifts directly from shell-model results without introducing additional Berggren basis states as in NCGSM or additional RGM calculations as in the NCSM/RGM approach.

The SS-HORSE approach is based on a simple analysis of the $\hbar\Omega$ and basis-space dependencies of the results of standard variational shell-model calculations. We have successfully applied it to extracting resonance energies and widths in $n\alpha$ scattering as well as non-resonant $n\alpha$ elastic scattering phase shifts [30, 31] from the NCSM calculations of ^{5}He and ^{4}He nuclei with JISP16 NN interaction [35]. To describe democratic decays [36, 37] of few-nucleon systems, we developed a hyperspherical extension of the SS-HORSE method [38, 39]. An application of this extended SS-HORSE approach to the study of the four-neutron system (tetraneutron) [38–40] make it possible to obtain for the first time a low-energy tetraneutron resonance consistent with a recent experiment [41] with soft realistic NN interactions like JISP16 [35], Daejeon16 [42] and SRG-evolved chiral effective field theory (χEFT) NN interactions. On the other hand, the unperturbed χEFT Idaho N3LO interaction [43] does not support a tetraneutron resonance narrow enough to be detected experimentally but instead provides a low-lying virtual tetraneutron state [40]. This result provides a possible explanation why the tetraneutron resonance has not been obtained before in numerous theoretical studies with various NN interactions with a repulsive core.

In this contribution, we discuss an extension of the SS-HORSE method to the case of charged particle scattering. The SS-HORSE technique provides the S-matrix or scattering phase shifts in some energy interval above the threshold where the shell model calculations generate eigenstates with various $\hbar\Omega$ values and various basis truncations. Next we parametrize the S-matrix to obtain it in a wider energy interval and to locate its poles associated with resonances. We have shown [30, 31] that this parametrization should provide a correct description of low-energy phase shifts. The

phase shift parametrization utilized in Refs. [30–32] was derived from the symmetry properties of the S-matrix. However, due to the long-range Coulomb interaction in the case of charged particle scattering, the analytical properties of the S-matrix become much more complicated and cannot be used for its low-energy parametrization. In Ref. [33] we suggested a version of the SS-HORSE approach which utilizes the phase shift parametrization based on analytical properties of the partial scattering amplitude. In the case of charged particle scattering, instead of the partial scattering amplitude one can use the so-called renormalized Coulomb-nuclear amplitude [44, 45] which has similar analytical properties. This opens a route to the generalization of the SS-HORSE method to the case of the charged particle scattering proposed in Ref. [34] where we have verified this approach using a model problem of scattering of particles interacting by the Coulomb and a short-range potential. To calculate the Coulomb-nuclear phase shifts, we make use of the version of the HORSE formalism suggested in Ref. [46] and utilized later in our studies of Refs. [28, 29].

In this contribution we present the results of SS-HORSE calculations of proton-α resonant and non-resonant scattering phase shifts based on the *ab initio* NCSM results for ^{5}Li and ^{4}He nuclei obtained with the JISP16 [35] and a newer Daejeon16 [42] NN interaction derived from a χEFT inter-nucleon potential and better fitted to the description of light nuclei than JISP16. We search for the S-matrix poles to evaluate the energies and widths of resonant states in ^{5}Li nucleus. The NCSM-SS-HORSE calculations of the ^{5}He resonant states have been performed with the JISP16 interaction in Refs. [30, 31]. We present here also the results of the NCSM-SS-HORSE ^{5}He resonant state calculations with the Daejeon16 to complete the studies of the nucleon-α resonances with the realistic JISP16 and Daejeon16 NN potentials. The previous *ab initio* analyses of nucleon-α resonances with various modern realistic inter-nucleon interactions were performed in Ref. [26] within the GFMC and in Refs. [22, 47–49] within the NCSM/RGM.

2 SS-HORSE method for channels with neutral and charged particles

2.1 General formulae

The SS-HORSE approach relies on the J-matrix formalism in quantum scattering theory.

Originally, the J-matrix formalism was developed in atomic physics [50] [4]; therefore, the so-called Laguerre basis was naturally used within this approach. A generalization of this formalism utilizing either the Laguerre or the harmonic oscillator bases was suggested in Ref. [51]. Later the harmonic-oscillator version of the J-matrix method was independently rediscovered by Kiev (G. F. Filippov and collaborators) [52] and Moscow (Yu. F. Smirnov and collaborators) [53] groups. The J-matrix with oscillator basis is sometimes also referred to as an *Algebraic Version of RGM* [52] or as a *Harmonic Oscillator Representation of Scattering Equations* (HORSE) [46]. We use here a generalization of the HORSE formalism to the case of charged particle scattering proposed in Ref. [46].

Within the HORSE approach, the basis function space is split into internal and external regions. In the internal region which includes the basis states with oscillator quanta $N \leq \mathbb{N}$, the Hamiltonian completely accounts for the kinetic and potential

energies. The internal region can be naturally associated with the shell model basis space. In the external region, the Hamiltonian accounts for the relative kinetic energy of the colliding particles (and for their internal Hamiltonians if needed) only and its matrix takes a form of an infinite tridiagonal matrix of the kinetic-energy operator (plus the sum of eigenenergies of the colliding particles at the diagonal if they have an internal structure). The external region clearly represents the scattering channel under consideration. If the eigenenergies E_ν, $\nu = 0, 1, ...$ and the respective eigenvectors of the Hamiltonian matrix in the internal region are known, one can easily calculate the S-matrix, phase shifts and other parameters characterizing the scattering process (see, e. g., Refs. [46, 51, 54, 55]).

An interesting feature peculiar to the J-matrix method was highlighted as far back as 1974 [50]. The point is that, at the energies coinciding with the eigenvalues E_ν of the Hamiltonian matrix in the internal region, the matching condition of the J-matrix method becomes substantially simpler while the accuracy of the S-matrix and phase shift description at these energies is much better than at the energies far enough from the eigenvalues E_ν [34, 56, 57]. Taking an advantage of this feature, H. Yamani [57] was able to construct an analytic continuation to the complex energy plane within the R-matrix method and to obtain accurate estimates for the energies and widths of resonant states.

The Single-State HORSE (SS-HORSE) method suggested in Refs. [30–32] also benefits from the improved accuracy of the HORSE approach at the eigenstates of the Hamiltonian matrix truncated to the internal region of the whole basis space. In the case of scattering of uncharged particles interacting by a short-range potential, the phase shifts $\delta_l(E_\nu)$ in the partial wave with the orbital momentum l at the eigenenergies E_ν of the internal Hamiltonian matrix are given by [30–32]

$$\tan\delta_l(E_\nu) = -\frac{S_{\mathbb{N}+2,l}(E_\nu)}{C_{\mathbb{N}+2,l}(E_\nu)}. \tag{1}$$

Here $S_{N,l}(E)$ and $C_{N,l}(E)$ are respectively regular and irregular solutions of the free Hamiltonian at energy E in the oscillator representation which analytical expressions can be found in Refs. [46, 51, 54, 55]. Varying the oscillator basis spacing $\hbar\Omega$ and the truncation boundary $\mathbb{N}$ of the internal oscillator basis subspace, we obtain a variation of some eigenenergy E_ν of the truncated Hamiltonian matrix in some energy interval and obtain the phase shifts $\delta_l(E)$ in that energy interval by means of Eq. (1). Next we parametrize the phase shifts $\delta_l(E)$ as discussed in the next subsection to have the phase shifts and the S-matrix in a wider energy interval which makes it possible to locate the S-matrix poles.

In the case of scattering in the channels with two charged particles, we, following the ideas of Ref. [46], formally cut the Coulomb interaction at the distance $r = b$. As shown in Ref. [34], an optimal value of the Coulomb cutoff distance b is the so-called *natural channel radius* b_0 [46],

$$b = b_0 \equiv r^{cl}_{\mathbb{N}+2,l} = 2r_0\sqrt{\mathbb{N}/2 + 7/4}\,, \tag{2}$$

i. e., b is equivalent to the classical turning point $r^{cl}_{\mathbb{N}+2,l}$ of the first oscillator function $R_{\mathbb{N}+2,l}(r)$ in the external region of the basis space. The parameter $r_0 = \sqrt{\hbar/(\mu\Omega)}$ entering Eq. (2) is the oscillator radius and μ is the reduced mass in the channel under consideration. With this choice of the Coulomb cutoff distance b, the elements of the

Hamiltonian matrix in the internal region are insensitive to the cut of the Coulomb interaction. Therefore the shell model Hamiltonian matrix elements in the internal region can be calculated without any modification of the Coulomb interaction between the nucleons. The scattering phase shifts δ_l^{aux} of the auxiliary Hamiltonian with the cutted Coulomb interaction can be calculated using the standard HORSE or SS-HORSE technique, e. g., with the help of Eq. (1). To deduce an expression for the Coulomb-nuclear phase shifts δ_l, one should match at the distance b the plane-wave asymptotics of the auxiliary Hamiltonian wave functions with Coulomb-distorted wave function asymptotics. As a result, we get the following SS-HORSE expression for the Coulomb-nuclear phase shifts $\delta_l(E_\nu)$ at the eigenenergies E_ν of the internal Hamiltonian matrix [34]:

$$\tan\delta_l\big(E_\nu\big) = -\frac{S_{\mathbb{N}+2,l}\big(E_\nu\big)\, W_b(n_l,F_l) + C_{\mathbb{N}+2,l}(E_\nu)\, W_b(j_l,F_l)}{S_{\mathbb{N}+2,l}\big(E_\nu\big)\, W_b(n_l,G_l) + C_{\mathbb{N}+2,l}\big(E_\nu\big)\, W_b(j_l,G_l)}. \tag{3}$$

Here $j_l \equiv j_l(kr)$ and $n_l \equiv n_l(kr)$ are respectively the spherical Bessel and Neumann functions [58] while $F_l \equiv F_l(\eta,kr)$ and $G_l \equiv G_l(\eta,kr)$ are respectively the regular and irregular Coulomb functions [58]; k is the relative motion momentum; $\eta = Z_1Z_2e^2\mu/k$ is the Sommerfeld parameter; the quasi-Wronskian

$$W_b(\phi,\chi) = \left(\frac{d\phi}{dr}\,\chi \,-\, \phi\,\frac{d\chi}{dr}\right)\Bigg|_{r=b}. \tag{4}$$

As in the case of neutral particle scattering, we obtain the Coulomb-nuclear phase shifts $\delta_l(E)$ in some energy interval by varying the internal region boundary $\mathbb{N}$ and the oscillator basis spacing $\hbar\Omega$ and next parametrize the phase shifts to have them in a wider energy interval. However the phase shift parametrization is more complicated for channels with charged colliding particles as discussed below.

An important scaling property of variational calculations with the harmonic oscillator basis was revealed in Refs. [9,10]: the converging variational eigenenergies E_ν depend on $\hbar\Omega$ and $\mathbb{N}$ not independently but only through a scaling variable

$$s = \frac{\hbar\Omega}{\mathbb{N}+7/2}. \tag{5}$$

This scaling property was initially proposed in Refs. [9,10] for the bound states. We have extended the scaling to the case of variational calculations with the harmonic oscillator basis of the unbound states [30,31] within the SS-HORSE approach. The SS-HORSE extension to the case of charged particle scattering discussed here can be used to demonstrate that the long-range Coulomb interaction does not destroy the scaling property of the unbound states (see Ref. [34] for details).

2.2 Phase shift parametrization

The total partial-wave amplitude for scattering in the case of Coulomb and short-range interactions has the form of the sum of the purely Coulomb, $f_l^C(k)$, and Coulomb-nuclear, $f_l^{NC}(k)$, amplitudes [59],

$$f_l(k) = f_l^C(k) + f_l^{NC}(k), \tag{6}$$

which, in turn, are related to the purely Coulomb, $\sigma_l = \arg\Gamma(1+l+i\eta)$, and Coulomb-nuclear phase shifts, δ_l, as

$$f_l^C(k) = \frac{\exp(2i\sigma_l) - 1}{2ik}, \tag{7}$$

$$f_l^{NC}(k) = \exp(2i\sigma_l)\,\frac{\exp(2i\delta_l) - 1}{2ik}. \tag{8}$$

Analytic properties of the Coulomb-nuclear amplitude $f_l^{NC}(k)$ in the complex momentum plane differ from the analytic properties of the scattering amplitude for neutral particles. However, the *renormalized Coulomb-nuclear amplitude* [44, 45],

$$\widetilde{f}_l(E) = \frac{\exp(2i\delta_l) - 1}{2ik} \cdot \frac{\exp(2\pi\eta) - 1}{2\pi\eta}\, c_{l\eta}, \tag{9}$$

where

$$c_{l\eta} = \prod_{n=1}^{l} (1 + \eta^2/n^2)^{-1} \quad (l > 0), \qquad c_{0\eta} = 1, \tag{10}$$

is identical in analytic properties on the real momentum axis with the scattering amplitude for neutral particles. In particular, the renormalized amplitude can be expressed [44, 45]

$$\widetilde{f}_l = \frac{k^{2l}}{\widetilde{K}_l(E) - 2\eta k^{2l+1} H(\eta)(c_{l\eta})^{-1}} \tag{11}$$

in terms of the *Coulomb-modified effective-range function* [44, 45]

$$\widetilde{K}_l(E) = k^{2l+1}(c_{l\eta})^{-1}\left\{\frac{2\pi\eta}{\exp(2\pi\eta) - 1}\left[\cot\delta_l(k) - i\right] + 2\eta H(\eta)\right\}, \tag{12}$$

where

$$H(\eta) = \Psi(i\eta) + (2i\eta)^{-1} - \ln(i\eta), \tag{13}$$

$\Psi(z)$ is the logarithmic derivative of the Γ function (digamma or Ψ function) [58]. In the absence of Coulomb interaction ($\eta = 0$), the Coulomb-modified effective-range function transforms into the standard effective-range function for neutral particle scattering,

$$\widetilde{K}_l(E) = K_l(E) = k^{2l+1}\cot\delta_l, \tag{14}$$

while the renormalized amplitude becomes the conventional neutral particle scattering amplitude,

$$f_l(E) = \frac{k^{2l}}{K_l(E) - ik^{2l+1}}. \tag{15}$$

Due to their nice analytic properties, the renormalized Coulomb-nuclear amplitude, $\widetilde{f}_l(E)$, and the neutral particle scattering amplitude, $f_l(E)$, can be used to parametrize respectively the Coulomb-nuclear and neutral particle scattering phase shifts ensuring their correct low-energy behavior. In Refs. [33, 34], we introduced an auxiliary complex-valued function imbedding resonant pole parameters in the amplitude parametrization. These resonant pole parameters play a role of additional

fitting parameters in the phase-shift parametrization. Here we prefer to parametrize the Coulomb-modified effective-range function (12) or the standard effective-range function for neutral particle scattering (14) thus reducing the number of fit parameters. The resonant parameters are obtained by a numerical location of the amplitude pole as discussed below.

The Coulomb-modified effective-range function $\widetilde{K}_l(E)$ as well as the effective-range function for neutral particle scattering $K_l(E)$ is real on the real axis of momentum k, is regular in the vicinity of zero, and admits an expansion in even powers of k, or, equivalently, in power series of the relative motion energy $E = \hbar^2 k^2/2\mu$ [44, 45],

$$\widetilde{K}_l(E) = w_0 + w_1 E + w_2 E^2 + ... \tag{16}$$

The expansion coefficients w_0 and w_1 are related to the so-called scattering length a_l and effective range r_l [59]:

$$w_0 = -\frac{1}{a_l}, \quad w_1 = \frac{r_l \mu}{\hbar^2}. \tag{17}$$

We use the expansion coefficients w_0, w_1 and w_2 as fit parameters for the phase shift parametrization. Such a parametrization works well in the case of nucleon-α scattering but may fail in other problems. Note, as seen from Eq. (12) or Eq. (14), the energies at which the phase shift takes the values of 0, $\pm\pi$, $\pm 2\pi$, ..., are the singular points of the effective-range function. In the case of possible presence of such singular points in the range of energies of interest for a particular problem, one should use a more elaborate parametrization of the effective-range function, e. g., in the form of the Padé approximant.

2.3 Fitting process

In the case of neutral particle scattering, we combine Eqs. (1), (14) and (16) to obtain

$$w_0 + w_1 E + w_2 E^2 = k^{2l+1} \frac{C_{\mathbb{N}+2,l}(E)}{S_{\mathbb{N}+2,l}(E)}. \tag{18}$$

In the case of charged particle scattering, we derive a more complicated equation with the help of Eq. (3) and (12):

$$w_0 + w_1 E + w_2 E^2 = k^{2l+1} (c_{l\eta})^{-1}$$
$$\times \left\{ -\frac{2\pi\eta}{\exp(2\pi\eta) - 1} \left[\frac{S_{\mathbb{N}+2,l}(E)\, W_b(n_l, G_l) + C_{\mathbb{N}+2,l}(E)\, W_b(j_l, G_l)}{S_{\mathbb{N}+2,l}(E)\, W_b(n_l, F_l) + C_{\mathbb{N}+2,l}(E)\, W_b(j_l, F_l)} + i \right] + 2\eta H(\eta) \right\}. \tag{19}$$

Let $E_\nu^{(i)}$, $i = 1, 2, ..., D$, be a set of the lowest ($\nu = 0$) or some other particular eigenvalues ($\nu > 0$) of the Hamiltonian matrix truncated to the internal region of the basis space obtained with a set of parameters $(\mathbb{N}^{(i)}, \hbar\Omega^{(i)})$, $i = 1, 2, ..., D$. We find energies $\mathcal{E}^{(i)}$ as solutions of Eq. (18) or Eq. (19) with some trial set of the effective-range function expansion coefficients w_0, w_1, w_2 for each combination of parameters $(\mathbb{N}^{(i)}, \hbar\Omega^{(i)})$ [note, the oscillator basis parameter $\hbar\Omega$ enters definitions of

functions $S_{N,l}(E)$ and $C_{N,l}(E)$]. The optimal set of the fit parameters w_0, w_1, w_2 parametrizing the phase shifts is obtained by minimizing the functional

$$\Xi = \sqrt{\frac{1}{D}\sum_{i=1}^{D}\left(E_\nu^{(i)} - \mathcal{E}^{(i)}\right)^2}. \tag{20}$$

With the optimal set of the fit parameters w_0, w_1, w_2 we can use Eq. (18) or Eq. (19) to obtain the $\hbar\Omega$ dependences of the eigenenergies $E_\nu(\hbar\Omega)$ in any basis space $\mathbb{N}$. Therefore Eqs. (18) and (19) provide extrapolation of the variational results for unbound states to larger basis spaces.

2.4 Resonance energy E_r and width Γ

We obtain resonance energies E_r and widths Γ by a numerical location of the S-matrix poles which coincide with the poles of scattering amplitude. If the amplitude has a resonant pole at a complex energy $E = E_p$, the resonance energy E_r and its width Γ are related to the real and imaginary part of E_p [59]:

$$E_p = E_r - i\frac{\Gamma}{2}. \tag{21}$$

It follows from Eqs. (11) and (15) that locating the pole of the scattering amplitude is equivalent to solving in the complex energy plane the equation

$$\mathcal{F}(E) \equiv \widetilde{K}_l(E) - 2\eta k^{2l+1} H(\eta)(c_{l\eta})^{-1} = 0 \tag{22}$$

in the case of charged particle scattering or the equation

$$\mathcal{F}(E) \equiv K_l(E) - ik^{2l+1} = 0 \tag{23}$$

in the case of neutral particles. We can use the parametrization of functions $\widetilde{K}_l(E)$ or $K_l(E)$ in Eqs. (22) and (23). To solve these equations, we calculate the integral

$$\Upsilon = \frac{1}{2\pi i}\oint\limits_C \frac{\mathcal{F}'(E)}{\mathcal{F}(E)}\,dE \tag{24}$$

along some closed contour C in the complex energy plane, where $\mathcal{F}'(E) = \frac{d\mathcal{F}}{dE}$. The contour C should surround the area where we expect to have the pole of the amplitude. According to the theory of functions of a complex variable [60], the value of Υ is equal to the number of zeroes of the function $\mathcal{F}(E)$ in the area surrounded by the contour C. If needed, we modify the contour C to obtain

$$\Upsilon = 1. \tag{25}$$

The position of the pole in the energy plane is calculated as

$$E_p = \frac{1}{2\pi i}\oint\limits_C E\,\frac{\mathcal{F}'(E)}{\mathcal{F}(E)}\,dE. \tag{26}$$

A numerical realization of the algorithm based on Eqs. (24)–(26) provides fast and stable locating of the poles of scattering amplitude.

3 Elastic scattering of nucleons by α particle in the NCSM-SS-HORSE approach

We present here an application of our SS-HORSE technique to nucleon-α scattering phase shifts and resonance parameters based on *ab initio* many-body calculations of ^{5}He and ^{5}Li nuclei within the NCSM with the realistic JISP16 and Daejeon16 NN interactions. The NCSM calculations are performed using the code MFDn [61,62] with basis spaces including all many-body oscillator states with excitation quanta $N_{\max}$ ranging from 2 up to 18 for both parities and with $\hbar\Omega$ values ranging from 10 to 40 MeV in steps of 2.5 MeV.

Note, for the NCSM-SS-HORSE analysis we need the ^{5}He and ^{5}Li energies relative respectively to the $n+\alpha$ and $p+\alpha$ thresholds. Therefore from each of the ^{5}He or ^{5}Li NCSM odd (even) parity eigenenergies we subtract the ^{4}He ground state energy obtained by the NCSM with the same $\hbar\Omega$ and the same $N_{\max}$ (with $N_{\max}-1$) excitation quanta, and in what follows these subtracted energies are referred to as the NCSM eigenenergies E_ν. Only these ^{5}He and ^{5}Li NCSM eigenenergies relative to the respective threshold are discussed below.

We note here that the NCSM utilizes the truncation based on the many-body oscillator quanta $N_{\max}$ while the SS-HORSE requires the oscillator quanta truncation of the interaction describing the relative motion of nucleon and α particle. A justification of using $N_{\max}$ for the SS-HORSE analysis is obvious if the α particle is described by the simplest four-nucleon oscillator function with excitation quanta $N^\alpha_{\max}=0$. Physically it is clear that the use of $N_{\max}$ within the SS-HORSE should work well also in a more general case when the α particle is presented by the wave function with $N^\alpha_{\max}>0$ due to the dominant role of the zero-quanta component in the α particle wave function. Instead of attempting to justify algebraically the use of $N_{\max}$ within the SS-HORSE, we suggested in Ref. [30,31] an *a posteriori* justification: we demonstrated in Ref. [30,31] that we obtained $n\alpha$ phase shift parametrizations consistent with the NCSM results obtained with very different $N_{\max}$ and $\hbar\Omega$ values; more, we were able to predict the NCSM results with large $N_{\max}$ using the phase shift parametrizations based on the NCSM calculations with much smaller model spaces. It was clearly impossible if the use of $N_{\max}$ truncation for the SS-HORSE analysis did not work properly. We perform the same *a posteriori* analysis of our results in this study of nucleon-α scattering to ensure the justification of our approach though do not present and discuss it below. Generally the fact that the phase shifts calculated using Eq. (1) or (3) at the NCSM eigenenergies obtained with different $N_{\max}$ truncations form a single curve as a function of energy serves as a confirmation of the consistency of the whole NCSM-SS-HORSE approach and of the use of the NCSM $N_{\max}$ for the SS-HORSE phase shift calculation in particular. The ranges of $N_{\max}$ and $\hbar\Omega$ values where this consistency is achieved differ for different NN interactions and different angular momenta and parities. Such a consistency which can be also interpreted as a convergence of the phase shift calculations is seen in the figures below to be achieved in all calculations at least at largest basis spaces in some range of $\hbar\Omega$ values.

3.1 Phase shifts of resonant $p\alpha$ scattering

The top left panel of Fig. 1 presents the results of the NCSM calculations of the ^{5}Li $\frac{3}{2}^-$ ground state energies $E_0^{(i)}$ relative to the $p+\alpha$ threshold. The respective

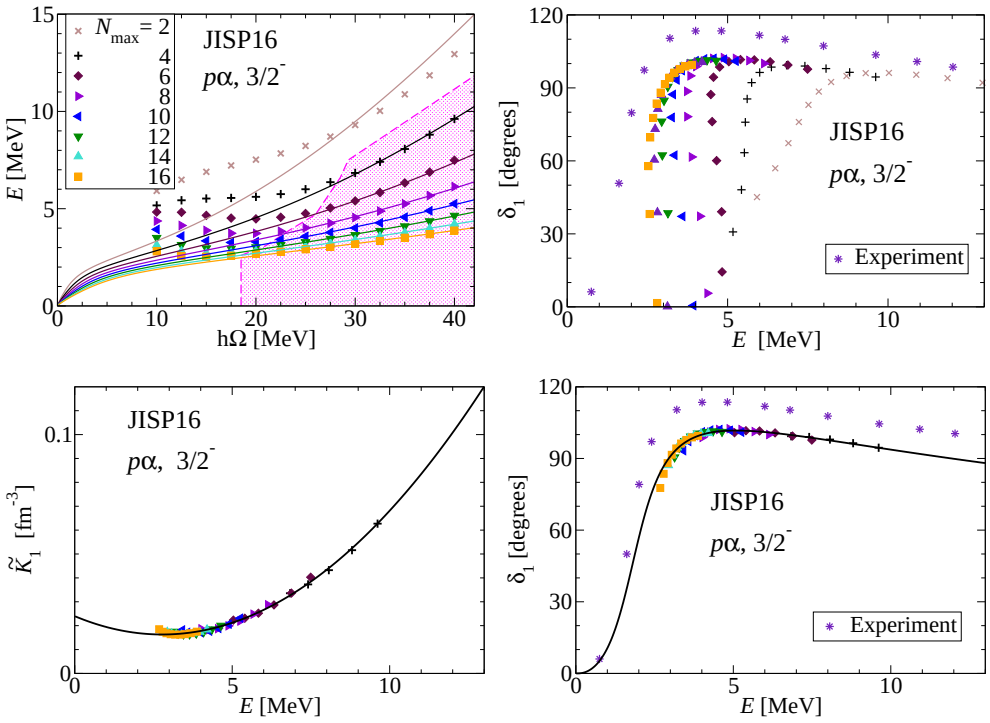

Figure 1: $p\alpha$ scattering in the $\frac{3}{2}^-$ state with JISP16 NN interaction. Top left: the lowest ^{5}Li $\frac{3}{2}^-$ eigenenergies $E_0^{(i)}$ relative to the $p+\alpha$ threshold obtained by the NCSM with various $N_{\max}$ (symbols) as functions of $\hbar\Omega$. The shaded area shows the energy values selected for the SS-HORSE analysis. Solid curves are solutions of Eq. (19) for energies E with parameters w_0, w_1 and w_2 obtained by the fit. Top right: the $\frac{3}{2}^-$ $p\alpha$ phase shifts obtained directly for all calculated ^{5}Li eigenstates $E_0^{(i)}$ using Eq. (3). Bottom left: Coulomb-modified effective range function $\widetilde{K}_l(E)$ calculated using Eq. (16) with parameters w_0, w_1 and w_2 obtained by the fit (solid curve) and calculated using the r.h.s. of Eq. (19) at the selected eigenenergies $E_0^{(i)}$ (symbols). Bottom right: the fit of the $\frac{3}{2}^-$ $p\alpha$ phase shifts (solid curve) and the phase shifts obtained directly from the selected ^{5}Li eigenstates $E_0^{(i)}$ using Eq. (3) (symbols). Experimental data at the right panels (stars) are taken from Ref. [63].

phase shifts calculated using Eq. (3) for all ^{5}Li eigenstates $E_0^{(i)}$ are shown in the top right panel of Fig. 1.

For the SS-HORSE analysis we should select a set of consistent (converged) NCSM eigenstates $E_0^{(i)}$ which form a single curve of the phase shifts $\delta_l\big(E_0^{(i)}\big)$ vs energy as discussed in detail in Refs. [30–34]. Alternatively one can use for the eigenstate selection the graph of $E_0^{(i)}$ vs the scaling parameter s or the graph of the Coulomb-modified effective range function points $\widetilde{K}_l\big(E_0^{(i)}\big)$ vs energy where the converged eigenstates should also form a single curve. Our selection of the eigenstates $E_0^{(i)}$ is illustrated by the shaded area in the top left panel of Fig. 1 while the method of the eigenstate

selection is seen from comparing the top right and bottom right panels in the same figure: the symbols in the top panel depict the phase shifts $\delta_1\big(E_0^{(i)}\big)$ corresponding to all eigenstates $E_0^{(i)}$ while those in the bottom panel correspond to the selected eigenstates only. More details regarding the eigenstate selection can be found in Refs. [30, 31] and we are not discussing the method of eigenstate selection in this paper in what follows.

A good quality of reproducing the Coulomb-modified effective range function points $\widetilde{K}_l\big(E_0^{(i)}\big)$ by the fit is illustrated by the bottom left panel in Fig. 1. We note the the quality of description by the fit of the functions $\widetilde{K}_l(E)$ and $K_l(E)$ in cases of other states and interactions is approximately the same and we shall not present the graphs of these functions in what follows. A numerical estimate of the fit quality in our approach is the rms deviation Ξ of the eigenenergies $E_0^{(i)}$ presented in Table 1. It is seen that in all cases Ξ is of the order of few tens of keV.

The bottom right panel in Fig. 1 demonstrates a good quality of the fit of the phase shift points $\delta_1\big(E_0^{(i)}\big)$. The fitted phase shifts are seen from this panel to be in a good correspondence with the results of the phase shift analysis of the experimental data of Ref. [63]. However the theoretical phase shift behavior indicates that the resonance has a slightly higher energy and a larger width than observed experimentally.

The results of the calculations of the same phase shifts with the Daejeon16 NN interaction are presented in Fig. 2. It is seen that in this case we reproduce the experimental phase shifts in the resonance region even better than with JISP16. However we can select for the SS-HORSE analysis much less NCSM results than in the case of JISP16: only the NCSM states obtained with Daejeon16 with $N_{\max} \geq 12$ are forming the same curve on the $\delta_1\big(E_0^{(i)}\big)$ vs energy plot while in the JISP16 case we utilize for the SS-HORSE analysis the results with $N_{\max} \geq 4$. In other words, surprisingly, the convergence of continuum state calculations with the Daejeon16 NN interaction is much worse than with JISP16 while the Daejeon16 results in a much faster convergence of NCSM calculations for bound states of light nuclei [42]. The same trends in comparing convergence of Daejeon16 and JISP16 continuum calculations are seen in all the rest results presented here.

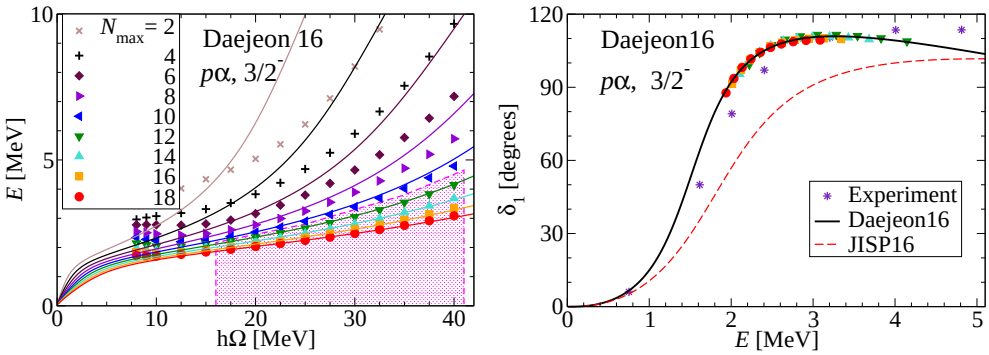

Figure 2: $p\alpha$ scattering in the $\frac{3}{2}^-$ state with Daejeon16 NN interaction. Dashed curve in the right panel presents phase shifts obtained with JISP16 for comparison. See Fig. 1 for other details.

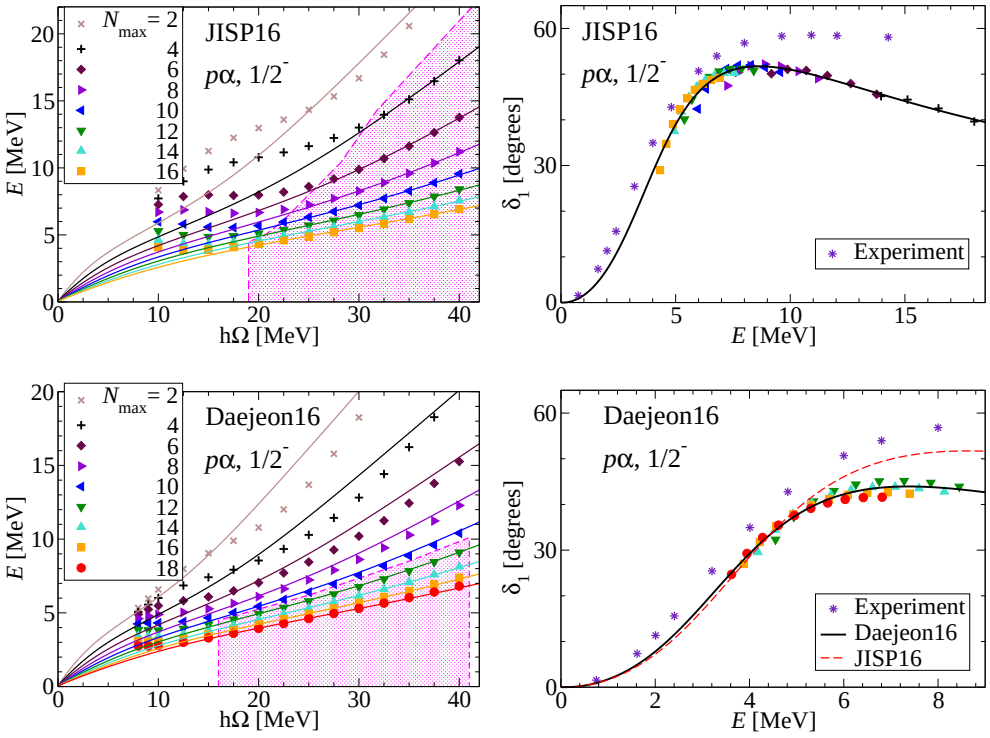

Figure 3: $p\alpha$ scattering in the $\frac{1}{2}^-$ state with JISP16 (top panels) and Daejeon16 (bottom panels) NN interactions. Dashed curve in the bottom right panel presents phase shifts obtained with JISP16 for comparison. See Fig. 1 for other details.

The results of calculations of the $p\alpha$ scattering in the $\frac{1}{2}^-$ state with JISP16 and Daejeon16 are presented in Fig. 3. Both interactions are reproducing well the experimental data in the resonance region while the JISP16 phase shifts are closer to the experiment at higher energies.

3.2 Phase shifts of resonant $n\alpha$ scattering

We have studied the $n\alpha$ scattering within the NCSM-SS-HORSE approach with the JISP16 NN interaction in Refs. [30,31]. We present for completeness the resonant $n\alpha$ phase shifts obtained with Daejeon16 in Fig. 4 in comparison with those from JISP16. As in the case of the $p\alpha$ scattering, the narrower $\frac{3}{2}^-$ resonance is better described by the Daejeon16 than by the JISP16 interaction while the description of the wider $\frac{1}{2}^-$ resonance region is nearly the same by both interaction but the $\frac{1}{2}^-$ phase shift behavior at energies above the resonant is reproduced better by JISP16. We note again a faster convergence of the JISP16 calculations of $n\alpha$ scattering phase shifts as compared with those with Daejeon16.

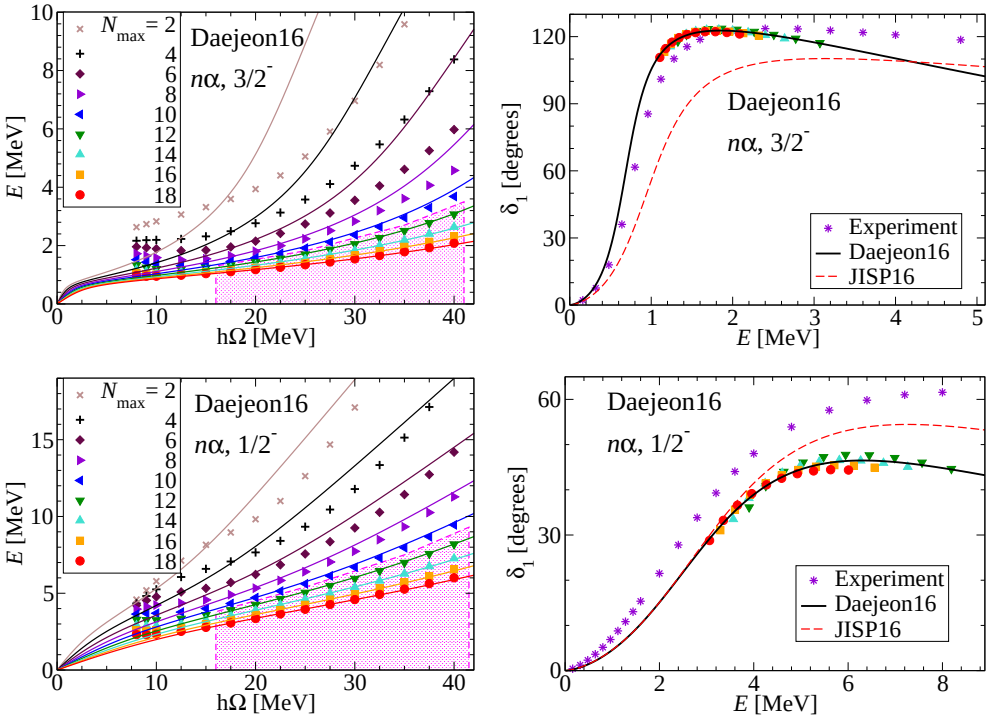

Figure 4: $n\alpha$ scattering in the $\frac{3}{2}^-$ (top panels) and $\frac{1}{2}^-$ (bottom panels) states with the Daejeon16 NN interaction. Dashed curves in the right panels present phase shifts obtained with JISP16 [30] for comparison. Experimental data (stars) are taken from Ref. [64]. See Fig. 1 for other details.

3.3 $\frac{3}{2}^-$ and $\frac{1}{2}^-$ resonances in ^{5}Li and ^{5}He nuclei

The results for energies and widths of the $\frac{3}{2}^-$ and $\frac{1}{2}^-$ resonances in ^{5}Li and ^{5}He nuclei with respect to the nucleon + α threshold obtained by the numerical location of the scattering amplitude poles as described in Subsection 2.4, are presented in Table 1. For comparison, we present in Table 1 also the results for the ^{5}Li resonances obtained with χEFT NN and NNN interactions in the *ab initio* NCSM/RGM approach in Ref. [49]. We note that the energy of the resonance was calculated in Ref. [49] as a position of the maximum of the derivative $\frac{d\delta_l(E)}{dE}$ while the resonance width was evaluated as $\Gamma = 2/(d\delta_l/dE)|_{E=E_r}$. The phase shift $\delta_l(E)$ may have a contribution from a non-resonant background which can result in some shift of the resonance energy E_r and in a modification of its width Γ in such calculations as compared with a more theoretically substantiated method relating the resonance parameters to the S-matrix and/or scattering amplitude pole. The differences in energy and width from these different type calculations may be large for wide resonances.

We note that all *ab initio* calculations of resonance parameters in ^{5}Li and ^{5}He nuclei provide a good description of the experimental data of Ref. [65]. The difference in $\frac{3}{2}^-$ resonance energies in both nuclei obtained with different interactions is less than 300 keV, and the experimental resonance energies are within the respective

Table 1: Energies E_r and widths Γ of resonant states $\frac{3}{2}^-$ and $\frac{1}{2}^-$ in ^{5}Li and ^{5}He obtained in the NCSM-SS-HORSE approach with JISP16 and Daejeon16 NN interactions. Ξ presents the rms deviation of energies obtained in the fit. The NCSM/RGM results obtained with χEFT NN and NNN interactions are from Ref. [49] and the experimental results are from Ref. [65].

	E_r (MeV)	Γ (MeV)	Ξ (keV)	E_r (MeV)	Γ (MeV)	Ξ (keV)	Δ (MeV)
	^{5}Li, $3/2^-$			^{5}Li, $1/2^-$			
Experiment	1.69	1.23		3.18	6.60		1.49
JISP16	1.80	1.79	45	3.57	6.09	65	1.77
Daejeon16	1.52	1.05	24	3.21	5.63	50	1.70
χEFT $NN+NNN$	1.77	1.70		3.11	7.90		1.34
	^{5}He, $3/2^-$			^{5}He, $1/2^-$			
Experiment	0.80	0.65		2.07	5.57		1.27
JISP16	0.94	1.02	40	2.63	5.31	62	1.69
Daejeon16	0.68	0.52	22	2.45	5.07	48	1.77

intervals of predictions obtained with different interactions. The theoretical predictions for the $\frac{3}{2}^-$ resonance widths also embrace the experimental values. However the spread of theoretical predictions for the $\frac{3}{2}^-$ resonance width is about 750 keV in the case of ^{5}Li and about 500 keV in the case of ^{5}He that are large numbers as compared with the width value.

In the case of the wider $\frac{1}{2}^-$ resonances in ^{5}Li and ^{5}He nuclei, the spreads of predictions for ^{5}Li also embrace the respective experimental energy and width values while our predictions for the ^{5}He resonance energy are slightly above and for the width are slightly below the experiment. However the spreads of the theoretical predictions for both energy and width of the $\frac{1}{2}^-$ resonances in ^{5}Li and ^{5}He do not exceed approximately 450 keV with an exception of the NCSM/RGM χEFT $NN+NNN$ prediction for the $\frac{1}{2}^-$ ^{5}Li resonance width. Even the 2.3 MeV difference between our Daejeon16 and χEFT $NN+NNN$ prediction of Ref. [49] for the $\frac{1}{2}^-$ ^{5}Li resonance width is much smaller than the experimental width. Therefore we can say that the relative accuracy of the *ab initio* predictions for the $\frac{1}{2}^-$ resonances in ^{5}Li and ^{5}He nuclei is much better than that for the $\frac{3}{2}^-$ resonances.

The difference $\Delta = \left(E_r^{1/2^-} - E_r^{3/2^-}\right)$ between the energies of the $\frac{1}{2}^-$ and $\frac{3}{2}^-$ resonances in ^{5}He and ^{5}Li nuclei can be associated with the spin-orbit splitting of respectively neutrons and protons in the p shell. The Δ values are presented in Table 1. The χEFT $NN+NNN$ interaction slightly underestimates the proton spin-orbit splitting while JISP16 and Daejeon16 overestimate both proton and neutron spin-orbit splittings. It is interesting to note that the differences between our predictions with JISP16 and Daejeon16 for the resonance energies are of the order of 300 keV while the differences in Δ values are only about 75 keV. It is more important to note that the charge-independent JISP16 and Daejeon16 NN interactions support nearly

the same p-shell spin-orbit splittings for protons and neutrons while the experimental spin-orbit splitting for protons exceeds that for neutrons by approximately 200 keV.

3.4 Non-resonant $p\alpha$ scattering

We have used the NCSM-SS-HORSE approach in Ref. [30–32] for calculations of resonant as well as non-resonant $n\alpha$ scattering. The non-resonant phase shifts can be also calculated within the current extension of the NCSM-SS-HORSE to the case of channels with charged colliding particles. Contrary to the phase shifts parametrizations based on the S-matrix analytic properties utilized on Ref. [30–32], we use the same Coulomb-modified effective-range function parametrization of Eq. (16) for both resonant and non-resonant scattering.

The results of calculations of the non-resonant $p\alpha$ scattering phase shifts in the $\frac{1}{2}^+$ state with JISP16 and Daejeon16 NN interactions are presented in Fig. 5. It is seen that JISP16 provides a faster convergence of the phase shifts in this case too. The results obtained with JISP16 and Daejeon16 are close to each other and reproduce well the experimental phase shifts of Ref. [63].

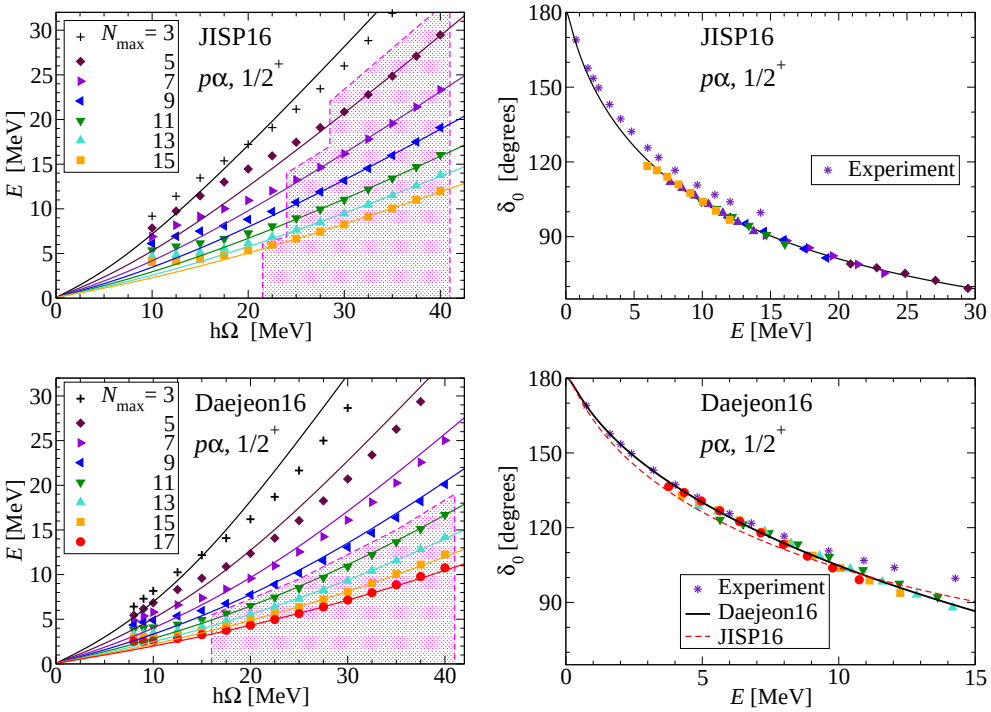

Figure 5: Non-resonant $p\alpha$ scattering in the $\frac{1}{2}^+$ state with JISP16 (top panels) and Daejeon16 (bottom panels) NN interactions. Dashed curve in the bottom right panel presents phase shifts obtained with JISP16 for comparison. See Fig. 1 for other details.

4 Summary

We present here an extension of the *ab initio* NCSM-SS-HORSE approach to the case of channels with charged colliding particles where the relative motion wave function asymptotics is distorted by the Coulomb interaction. The extended approach is applied to the study of $p\alpha$ scattering and resonances in ^{5}Li nucleus with realistic JISP16 and Daejeon16 NN interaction. The analysis of the $n\alpha$ scattering and resonances in ^{5}He nucleus with JISP16 NN interaction has been performed by us in Ref. [30–32]; we complete this analysis here by the corresponding calculations with Daejeon16.

We demonstrate that the extended NCSM-SS-HORSE approach works with approximately the same accuracy and convergence rate as its non-extended version applicable to the channels with neutral particles. Surprisingly, we obtain that the JISP16 interaction provides a faster convergence of the $n\alpha$ and $p\alpha$ phase shifts than the Daejeon16 while the convergence of bound states in light nuclei within NCSM is much faster with Daejeon16 than with JISP16 [42].

Both JISP16 and Daejeon16 provide a good description of the $\frac{3}{2}^-$ and $\frac{1}{2}^-$ resonances in ^{5}Li and ^{5}He nuclei as well as of the $\frac{1}{2}^+$ non-resonant $n\alpha$ and $p\alpha$ phase shifts. However the spin-orbit splitting of nucleons in the p shell is overestimated by these interactions; more, these charge-independent NN interactions provide nearly the same result for the spin-orbit splitting of neutrons and protons while experimentally the spin-orbit splittings for neutrons and protons differ by approximately 200 keV.

Acknowledgments

We are thankful to V. D. Efros and P. Maris for valuable discussions.

This work is supported in part by the Russian Foundation for Basic Research under Grant No. 15-02-06604-a and No. 16-02-00049-a, by the U.S. Department of Energy under Grants No. DESC00018223 (SciDAC/NUCLEI) and No. DE-FG02-87ER40371, by the US National Science Foundation under Grant No. 1516181, by the Rare Isotope Science Project of Institute for Basic Science funded by Ministry of Science and ICT and National Research Foundation of Korea (2013M7A1A1075764). Computational resources were provided by the National Energy Research Scientific Computing Center (NERSC), which is supported by the Office of Science of the U.S. Department of Energy under Contract No. DE-AC02-05CH11231, and by the Supercomputing Center/Korea Institute of Science and Technology Information including technical support (KSC-2015-C3-003).

References

[1] W. Leidemann and G. Orlandini, Prog. Part. Nucl. Phys. **68**, 158 (2013).

[2] S. C. Pieper and R. B. Wiringa, Ann. Rev. Nucl. Part. Sci. **51**, 53 (2001).

[3] B. R. Barrett, P. Navrátil and J. P. Vary, Prog. Part. Nucl. Phys. **69**, 131 (2013).

[4] H. Kümmela, K. H. Lührmann and J. Zabolitzky, Phys. Rep. **36**, 1 (1978).

[5] G. Hagen, D. J. Dean, M. Hjorth-Jensen, T. Papenbrock and A. Schwenk, Phys. Rev. C **76**, 044305 (2007).

[6] D. Lee, Prog. Part. Nucl. Phys. **63**, 117 (2009).

[7] E. Epelbaum, H. Krebs, D. Lee and U. G. Meissner, Phys. Rev. Lett. **106**, 192501 (2011).

[8] P. Maris, J. P. Vary and A. M. Shirokov, Phys. Rev. C **79**, 014308 (2009).

[9] S. A. Coon, M. I. Avetian, M. K. G. Kruse, U. van Kolck, P. Maris and J. P. Vary, Phys. Rev. C **86**, 054002 (2012).

[10] S. A. Coon, in *Proc. Int. Workshop Nucl. Theor. Supercomputing Era (NTSE-2012), Khabarovsk, Russia, June 18–22, 2012*, eds. A. M. Shirokov and A. I. Mazur. Pacific National University, Khabarovsk, 2013, p. 171, http://www.ntse-2012.khb.ru/Proc/S_Coon.pdf.

[11] R. J. Furnstahl, G. Hagen and T. Papenbrock, Phys. Rev. C **86**, 031301(R) (2012).

[12] S. N. More, A. Ekstrom, R. J. Furnstahl, G. Hagen and T. Papenbrock, Phys. Rev. C **87**, 044326 (2013).

[13] M. K. G. Kruse, E. D. Jurgenson, P. Navrátil, B. R. Barrett and W. E. Ormand, Phys. Rev. C **87**, 044301 (2013).

[14] D. Sääf and C. Forssén, Phys. Rev. C **89**, 011303 (2014).

[15] R. J. Furnstahl, S. N. More and T. Papenbrock, Phys. Rev. C **89**, 044301 (2014).

[16] S. König, S. K. Bogner, R. J. Furnstahl, S. N. More and T. Papenbrock, Phys. Rev. C **90**, 064007 (2014).

[17] R. J. Furnstahl, G. Hagen, T. Papenbrock and K. A. Wendt, J. Phys. G **42**, 034032 (2015).

[18] K. A. Wendt, C. Forssén, T. Papenbrock and D. Sääf, Phys. Rev. C **91**, 061301 (2015).

[19] S. A. Coon and M. K. G. Kruse, Int. J. Mod. Phys. E **25**, 1641011 (2016).

[20] L. D. Faddeev and S. P. Merkuriev, *Quantum scattering theory for several particle systems*. Kluwer, Dordrecht, 1993.

[21] E. O. Alt, P. Grassberger and W. Sandhas, Nucl. Phys. B **2**, 167 (1967).

[22] P. Navrátil, R. Roth and S. Quaglioni, Phys. Rev. C **82**, 034609 (2010).

[23] P. Navrátil, S. Quaglioni, I. Stetcu, B. R. Barrett, J. Phys. G **36**, 083101 (2009).

[24] P. Navrátil, S. Quaglioni, G. Hupin, C. Romero-Redondo and A. Calci, Phys. Scr. **91**, 053002 (2016).

[25] V. D. Efros, W. Leidemann, G. Orlandini and N. Barnea, J. Phys. G **34**, R459 (2007).

[26] K. M. Nollett, S. C. Pieper, R. B. Wiringa, J. Carlson and G. M. Hale, Phys. Rev. Lett. **99**, 022502 (2007).

[27] G. Papadimitriou, J. Rotureau, N. Michel, M. Płoszajczak and B. R. Barrett, Phys. Rev. C **88**, 044318 (2013).

[28] A. M. Shirokov, A. I. Mazur, J. P. Vary and E. A. Mazur, Phys. Rev. C **79**, 014610 (2009).

[29] A. M. Shirokov, A. I. Mazur, E. A. Mazur and J. P. Vary, Appl. Math. Inf. Sci. **3**, 245 (2009).

[30] A. M. Shirokov, A. I. Mazur, I. A. Mazur and J. P. Vary, Phys. Rev. C **94**, 064320 (2016).

[31] A. I. Mazur, A. M. Shirokov, I. A. Mazur and J. P. Vary, in *Proc. Int. Conf. Nucl. Theor. Supercomputing Era (NTSE-2014), Khabarovsk, Russia, June 23–27, 2014*, eds. A. M. Shirokov and A. I. Mazur. Pacific National University, Khabarovsk, 2016, p. 183, http://www.ntse-2014.khb.ru/Proc/A.Mazur.pdf.

[32] I. A. Mazur, A. M. Shirokov, A. I. Mazur and J. P. Vary, Phys. Part. Nucl. **48**, 84 (2017).

[33] L. D. Blokhintsev, A. I. Mazur, I. A. Mazur, D. A. Savin and A. M. Shirokov, Yad. Fiz. **80**, 102 (2017) [Phys. Atom. Nucl. **80**, 226 (2017)].

[34] L. D. Blokhintsev, A. I. Mazur, I. A. Mazur, D. A. Savin and A. M. Shirokov, Yad. Fiz. **80**, 619 (2017) [Phys. Atom. Nucl. **80**, 1093 (2017)].

[35] A. M. Shirokov, J. P. Vary, A. I. Mazur and T. A. Weber, Phys. Lett. B **644**, 33 (2007); a Fortran code generating the JISP16 matrix elements is available at http://lib.dr.iastate.edu/energy_datasets/2/.

[36] R. I. Jibuti and N. B. Krupennikova, *The method of hyperspherical functions in the quantum mechanics of few bodies*. Metsniereba, Tbilisi, 1984 (*in Russian*).

[37] R. I. Jibuti, Fiz. Elem. Chastits At. Yadra **14**, 741 (1983).

[38] A. M. Shirokov, G. Papadimitriou, A. I. Mazur, I. A. Mazur, R. Roth and J. P. Vary, in *Proc. Int. Conf. Nucl. Theor. Supercomputing Era (NTSE-2014), Khabarovsk, Russia, June 23–27, 2014*, eds. A. M. Shirokov and A. I. Mazur. Pacific National University, Khabarovsk, 2016, p. 174, http://www.ntse-2014.khb.ru/Proc/Shirokov.pdf.

[39] A. M. Shirokov, G. Papadimitriou, A. I. Mazur, I. A. Mazur, R. Roth and J. P. Vary, Phys. Rev. Lett. **117**, 182502 (2016).

[40] I. A. Mazur, A. M. Shirokov, A. I. Mazur, I. J. Shin, Y. Kim and J. P. Vary, *see these Proceedings*, p. 280, http://www.ntse-2016.khb.ru/Proc/IMazur.pdf.

[41] K. Kisamori *et al.*, Phys. Rev. Lett. **116**, 052501 (2016).

[42] A. M. Shirokov, I. J. Shin, Y. Kim, M. Sosonkina, P. Maris and J. P. Vary, Phys. Lett. B **761**, 87 (2016); a Fortran code generating the Daejeon16 matrix elements is available at http://lib.dr.iastate.edu/energy_datasets/1/.

[43] D. R. Entem and R. Machleidt, Phys. Lett. B **524**, 93 (2002); Phys. Rev. C **68**, 041001(R) (2003).

[44] J. Hamilton, I. Øverbö and B. Tromborg, Nucl. Phys. B **60**, 443 (1973).

[45] H. van Haeringen, *Charged-particle interactions. Theory and formulas.* Coulomb Press Leyden, Leiden, 1985.

[46] J. M. Bang, A. I. Mazur, A. M. Shirokov, Yu. F. Smirnov and S. A. Zaytsev, Ann. Phys. (NY) **280**, 299 (2000).

[47] S. Quaglioni and P. Navrátil, Phys. Rev. C **79**, 044606 (2009).

[48] G. Hupin, J. Langhammer, P. Navrátil, S. Quaglioni, A. Calci and R. Roth, Phys. Rev. C **88**, 054622 (2013).

[49] G. Hupin, S. Quaglioni and P. Navrátil, Phys. Rev. C **90**, 061601(R) (2014).

[50] E. J. Heller and H. A. Yamani, Phys. Rev. A **9**, 1201 (1974).

[51] H. A. Yamani and L. J. Fishman, J. Math. Phys, **16**, 410 (1975).

[52] G. F. Filippov and I. P. Okhrimenko, Yad. Fiz. **32**, 932 (1980) [Sov. J. Nucl. Phys. **32**, 480 (1980)]; G. F. Filippov, Yad. Fiz. **33**, 928 (1981) [Sov. J. Nucl. Phys. **33**, 488 (1981)].

[53] Yu. F. Smirnov and Yu. I. Nechaev, Kinam **4**, 445 (1982); Yu. I. Nechaev and Yu. F. Smirnov, Yad. Fiz. **35**, 1385 (1982) [Sov. J. Nucl. Phys. **35**, 808 (1982)].

[54] A. M. Shirokov, Yu. F. Smirnov and S. A. Zaytsev, in *Modern problems in quantum theory*, eds. V. I. Savrin and O. A. Khrustalev. Moscow State University, Moscow, 1998, p. 184.

[55] S. A. Zaytsev, Yu. F. Smirnov and A. M. Shirokov, Teor. Mat. Fiz. **117**, 227 (1998) [Theor. Math. Phys. **117**, 1291 (1998)].

[56] H. A. Yamani and M. S. Abdelmonem, J. Phys. A **26**, L1183 (1993).

[57] H. A. Yamani, Eur. J. Phys. **34**, 1025 (2013).

[58] M. Abramowitz and I. A. Stegun (eds.), *Handbook on mathematical functions.* Dover, New York, 1972; NIST digital library of mathematical functions, http://dlmf.nist.gov/.

[59] R. G. Newton, *Scattering theory of waves and particles, 2nd. ed.* Springer-Verlag, New York, 1982.

[60] A. G. Sveshnikov and A. N. Tikhonov, *The theory of functions of a complex variable, 2nd. ed.* Mir Publishers, Moscow, 1978.

[61] P. Maris, M. Sosonkina, J. P. Vary, E. G. Ng and C. Yang, Proc. Comput. Sci. **1**, 97 (2010).

[62] H. M. Aktulga, C. Yang, E. G. Ng, P. Maris and J. P. Vary, Concurrency Computat.: Pract. Exper. **26**, 2631 (2014).

[63] D. C. Dodder, G. M. Hale, N. Jarmie, J. H. Jett, P. W. Keaton, Jr., R. A. Nisley and K. Witte, Phys. Rev. C **15**, 518 (1977).

[64] R. A. Arndt, D. D. Long and L. D. Roper, Nucl. Phys. A **209**, 429 (1973).

[65] A. Csótó and G. M. Hale, Phys. Rev. C **55**, 536 (1997).